Carbohydrate Polymers 101 (2014) 1–10

Contents lists available at ScienceDirect

Carbohydrate Polymers

journal homepage: www.elsevier.com/locate/carbpol

Ultradrawing novel ultra-high molecular weight polyethylene fibers filled with bacterial cellulose nanofibers

Jen-taut Yeh[a,b,c,d,*], Chih-Chen Tsai[b], Chuen-Kai Wang[b], Jhih-Wun Shao[b], Ming-Zheng Xiao[a], Su-chen Chen[e]

[a] Hubei Collaborative Innovation Center for Advanced Organic Chemical Materials, Ministry of Education, Key Laboratory for the Green Preparation and Application of Functional Materials, Faculty of Materials Science and Engineering, Hubei University, Wuhan, China
[b] Graduate School of Material Science and Engineering, National Taiwan University of Science and Technology, Taipei, Taiwan
[c] Key Laboratory of Green Processing and Functional Textiles of New Textile Materials (Wuhan University of Science and Engineering), Ministry of Education, Wuhan, China
[d] School of Printing and Packaging, Wuhan University, Wuhan, China
[e] Taiwan Textile Research Institute, New Taipei City, Taiwan

ARTICLE INFO

Article history:
Received 11 May 2013
Received in revised form 12 July 2013
Accepted 15 August 2013
Available online 23 August 2013

Keywords:
Ultradrawing
Bacterial cellulose
Ultrahigh molecular weight polyethylene

ABSTRACT

Novel ultrahigh molecular weight polyethylene (UHMWPE)/bacterial cellulose (BC) ($F_{100}BC_y$) and UHMWPE/modified bacterial cellulose (MBC) ($F_{100}MBC_{x-y}$) as-prepared fibers were prepared and ultradrawn. The achievable draw ratio (D_{ra}) values of each $F_{100}MBC_{x-y}$ as-prepared fiber series specimens approached a maximum value as their MBC contents reached the optimal value at 0.0625 phr. In which, the maximum D_{ra} value obtained for $F_{100}MBC_{x-0.0625}$ as-prepared fiber specimen prepared at the optimal MBC content reached another maximum value at 347 as the weight ratio of maleic anhydride grafted polyethylene to BC approach an optimal value at 10. In contrast, no significant improvement in D_{ra} values was found for $F_{100}BC_y$ as-prepared fiber specimens. To understand these interesting ultradrawing properties described above, Fourier transform infra-red, specific surface areas, and transmission electron microcopic analyses of original and modified BC nanofibers together with the thermal, orientation and tensile properties of $F_{100}BC_y$ and $F_{100}MBC_{x-y}$ fiber specimens were performed.

1. Introduction

Polyethylene (Darras, Sequela, & Rietsch, 1992; Jiang, Lin, Chen, & Yeh, 2003; Kajiwara & Mcintyre, 1994; Kalb & Pennings, 1980a, 1980b; Kanamoto, Tsurta, Tanana, Takeda, & Porter, 1988; Kavesh & Prevorsek, 1983, 1985a, 1985b; Matsuo, Sawatari, Iida, & Yoneda, 1985; Ohta, 1983; Prevorsek, 1982; Sawatari, Okumura, & Matsuo, 1986; Smith, Chanzy, & Rotzinger, 1985; Smith, Chanzy, & Rotzinger, 1987; Smith & Lemstra, 1979, 1980a, 1980b; Smook & Pennings, 1982; Technical, 1996; Wilding & Word, 1978; Yeh & Chang, 2000, 2001, 2002; Yeh & Wu, 1998; Yeh, Chang, & Yen, 1998; Yeh, Lin, & Chen, 2003a; Yeh, Lin, & Chen, 2003b; Yeh, Lin, & Chen, 2003c; Yeh, Du, Lin, Hsie, & Chang, 2008; Yeh, Lin, Chen, & Huang, 2008; Yeh, Lin, & Fan-Chiang, 1996; Yeh et al., 2011a, 2011b, 2011c, 2013; Yeh, Wang, Hu, Lai, & Tsai, 2012), Polypropylene (Abo, Maaty, Olley, & Bassett, 1999; Mastuo, Sawatari, & Nakano, 1986) and Poly(vinyl alcohol) (Cha, Hyon, & Ikada, 1994; Yamaura et al., 1990; Yamaura, Suzuki, Yamamoto, Shimada, & Tanigami, 1995) fibers are typical high performance fibers produced using the gel spinning processing method from flexible polymer chains. Remarkable progress has been made in the improvement of these high performance fibers since then, however, the highest tensile strengths and moduli achieved for these fibers are still well below the broad range of theoretical tensile strengths and moduli reported for the perfect crystals of these polymers, respectively (Kajiwara & Mcintyre, 1994). The highest tenacity of commercially available UHMWPE fibers reaches as high as 45 g/den, which is about 10 times higher than those of steel fibers (Technical, 1996). However, this obtained strength is still far below the theoretical achievable strength, 372 g/den reported for the perfect polyethylene crystal (Ohta, 1983). The key element in obtaining high-strength UHMWPE fibers is to find a way to draw the as-prepared gel specimens to an ultrahigh draw ratio after the gel spinning process. The drawability of the as-prepared gel specimens was found to depend significantly on the compositions of solutions from which gels were made (Darras et al., 1992; Sawatari et al., 1986; Yeh & Chang, 2000, 2001, 2002; Yeh & Wu, 1998; Yeh et al., 1996, 1998, 2003a). Several

* Corresponding author at: Hubei Collaborative Innovation Center for Advanced Organic Chemical Materials, Ministry of Education, Key Laboratory for the Green Preparation and Application of Functional Materials, Faculty of Materials Science and Engineering, Hubei University, Wuhan, China. Tel.: +886 22737 6518.
E-mail address: jyeh@mail.ntust.edu.tw (J.-t. Yeh).

0144-8617/$ – see front matter © 2013 Elsevier Ltd. All rights reserved.
http://dx.doi.org/10.1016/j.carbpol.2013.08.034

authors (Jiang et al., 2003; Kanamoto et al., 1988; Matsuo et al., 1985; Smith & Lemstra, 1980a, 1980b; Smook & Pennings, 1982; Yeh & Chang, 2002; Yeh et al., 1998, 2003b) reported that the drawing temperature and rate could markedly affect the maximal achievable draw ratio and tensile properties of solution-grown UHMWPE samples. In addition to the gel solution compositions and drawing conditions, it is generally recognized that the conditions used in the formation process after spinning and/or solution casting of gel solutions can also have a significant influence on the morphology, microstructure and drawing properties of the specimens formed during the above mentioned processes (Kalb & Pennings, 1980b; Kavesh & Prevorsek, 1983, 1985a, 1985b; Prevorsek, 1982; Smith & Lemstra, 1979, 1980a, 1980b; Smook & Pennings, 1982; Wilding & Word, 1978; Yeh & Chang, 2002; Yeh et al., 2003c).

Our recent investigations (Yeh, Du et al., 2008; Yeh et al., 2011a, 2011b, 2011c, 2012, 2013) found that the achievable draw ratios (D_{ra}) of UHMWPE/nanofillers as-prepared fibers prepared near the optimal UHMWPE concentration improve to a maximal value as their nanofillers contents increase up to an optimal value, respectively. In which, the nanofillers (e.g. carbon nanotube (CNT) (Yeh, Du et al., 2008; Yeh, Lin, et al., 2008; Yeh et al., 2011a, 2011b, 2011c), attapulgite (ATP) (Yeh et al., 2012), nanosilica and/or their modified nanofillers (Yeh et al., 2013)) with extremely high specific surface areas ($\geq 150\,m^2\,g^{-1}$) can serve as efficient nucleation sites and facilitate the crystallization of UHMWPE molecules into crystals but with lower melting temperatures (T_m) and/or evaluated smaller crystal thickness (l_c) values during their crystallization processes. Presumably, the crystals with lower T_m and/or evaluated smaller l_c values obtained at proper plain and/or modified nanofiller contents can be melted and pulled out of folded lamellar crystals relatively easily during ultradrawing processes, and hence, results in higher drawability and orientation of the UHMWPE/nanofillers or UHMWPE/modified nanofillers as-prepared fibers. The maximal achievable draw ratios of UHMWPE/nanofillers or UHMWPE/modified nanofillers as-prepared series fiber specimens and the tensile strengths of the drawn UHMWPE/nanofillers or UHMWPE/modified nanofillers fiber specimens are significantly higher than those of the plain UHMWPE as-prepared and drawn fiber specimens prepared at the same draw ratios, UHMWPE concentrations but without addition of the nanofillers, respectively. The ultimate tensile strength values of the UHMWPE/purified ATP, UHMWPE/functionalized CNT and UHMWPE/functionalized nanosilica drawn fibers prepared using one-stage drawing process at 95 °C can reach 4.7, 5.8 and 7.0 GN m^{-2}, respectively, which is about 57, 93 and 133% higher than that of the corresponding plain UHMWPE drawn fibers prepared at the same optimal UHMWPE concentration, formation and drawing condition but without incorporation of modified nanofillers. These results clearly suggest that inorganic nanofillers with extremely high specific surface areas can act as efficient nucleation sites and significantly improve the achievable draw ratios and ultimate tenacity properties of nanofillers filled UHMWPE fibers.

Cellulose is one of the most copious polymers on the planet earth and is the main cell-wall component of just about every plant. It is a classic example of reinforcing elements for polymeric composites due to its high specific strength, modulus, biodegradability, high availability and low density (Choi, Mori, & Ohama, 2006; Cyras, Lannace, Kenny, & Vazquez, 2001; Thwe & Liao, 2002). Besides being the cell-wall component, cellulose is also secreted extracellularly as synthesized cellulose fibers by some bacterial species. Bacterial cellulose (BC) nanofibers can be metabolized by *Acetobacter xylinum* cultivated in a culture medium containing carbon and nitrogen sources (Embuscado, Marks, & BeMiller, 1994; Joseph, Thomas, & Pavithran, 1996; Suryanegara, Nakagaito, & Yano, 2009). It presents unique properties such as high mechanical strength and an extremely fine and pure fiber network structure. This network structure is in the form of a pellicle made up of a random assembly of ribbon-shaped fibrils, less than 100 nm wide, which are composed of a bundle of much finer microfibrils, 2 to 4 nm in diameter (Hwang, Yang, Hwang, Pyun, & Kim, 1999). Most recently, BC nanofibers were reported as an efficient reinforcing additive for preparing polymeric nanocomposites (Cristian et al., 2009; Gilkes, Kilburn, Miller, & Warren, 1991; Kurosumi, Sasaki, Yamashita, & Nakamura, 2002; Okiyama, Motoki, & Yamanaka, 1993; Wan et al., 2009; Yamanaka et al., 1989). However, the cost of using BC fibers as reinforcing fibers in polymeric nanocomposites remains too high to use for many commercial applications. In contrast to inorganic CNT, ATP and silica nanofillers, BC nanofibers are organic nanofillers with comparably high specific surface areas. However, natural BC nanofibers have never been used as reinforced or functional nanofillers in UHMWPE composite fibers to enhance their ultradrawing and/or ultimate tensile properties.

In this study, original and modified BC nanofibers were added in UHMWPE gel solutions to improve the ultradrawing and ultimate tensile properties of UHMWPE/BC and UHMWPE/modified BC fibers. The D_{ra} values of UHMWPE/BC and UHMWPE/modified BC as-prepared fibers approached a maximum value as the original BC and/or modified BC nanofiber contents reached their corresponding optimal values, respectively. In which, the maximum D_{ra} and ultimate tensile strength values obtained for UHMWPE/modified BC as-prepared fiber specimens are even higher than that of the UHMWPE/purified ATP, UHMWPE/functionalized CNT and UHMWPE/functionalized nanosilica as-prepared fiber specimens prepared at the optimal nanofiller contents, respectively (Yeh, Du, et al., 2008; Yeh et al., 2011b, 2011c, 2012, 2013). Specific surface area, morphological and Fourier transform infrared analyses of the original and modified BC nanofibers and/or investigations of thermal, orientation factor, morphological and ultimate tensile properties of the as-prepared and drawn UHMWPE/BC and UHMWPE/modified BC fiber specimens were performed to understand the above improved ultradrawing properties of the UHMWPE/BC and UHMWPE/modified BC as-prepared fiber specimens.

2. Experimental

2.1. Materials and sample preparation

The UHMWPE resin used in this study is associated with a weight-average molecular weight (Mw) of 5.0×10^6, which was kindly supplied by Yung Chia Chemical Industrial Corporation, Kaohsiung, Taiwan. *A. xylinum* (BCRC 17742) was purchased from Bioresource Collection and Research Center, Hsinchu, Taiwan. Basic media were composed of 100 g sugar, 10 g yeast extract (Difco Laboratories, Detroit, USA), 5 g $CaCO_3$ and 1 L Distilled water, wherein the pH value of the basic media was adjusted to 5.0. The basic culture media were sterilized at 121 °C in an autoclave for 45 min, and then cooled to room temperature. The *A. xylinum* was then cultivated in the granular sugar at the optimum temperature at 30 °C, pH value at 5, sugar content at 12.7 wt% and an air flow rate of 1.25 m/sec for 14 days. After metabolism, the bacterial cellulose (BC) products were washed and stirred in a beaker with distilled water for 40 min, and then repeatedly washed with fresh distilled water ten times to remove bacterial cells, residual sugars, salts and other metabolites. The purified bacterial cellulose products were then dried in an oven at 80 for 24 h before further characterization. The BC nanofibers were oxidized with 20% aqueous solution of $NaIO_4$ to produce cellulose aldehyde and then washed with tap water to remove the excess $NaIO_4$. Maleic anhydride grafted Polyethylene(PE_{-g-MAH}) resin was used to

modify oxidized BC nanofibers prepared above, in which $PE_{-g\text{-}MAH}$ resin was purchased from Langfang Plastic Corporation, Langfang, China. The modified BC(MBC) nanofibers were prepared by grafting $PE_{-g\text{-}MAH}$ molecules onto oxidized BC nanofibers in ultrasonicated decalin solution at 80 °C for 1 h, in which 10% of Polyoxyethylene sorbitan monolaurate (Polysorbate 20) was added as the surfactant to improve the reaction of the hydroxyl groups of BC nanofibers with the maleic anhydride groups of $PE_{-g\text{-}MAH}$ molecules during their modification processes.Polysorbate 20 was purchased from First Chemical Manufacture Corporation, Taipei, Taiwan.

Varying contents of BC and MBC together with UHMWPE resin were dispersed and/or dissolved in decalin solvent at 135 °C for 1.5 h, in which 0.1% di-t-butyl-p-cresol was added as an antioxidant. The UHMWPE, UHMWPE/BC and UHMWPE/MBC gel solutions prepared above were then fed into a temperature-controlled hopper and kept as hot homogenized gel solutions before spinning. The hot homogenized gel solutions were then gel-spun using a conical die with an exit diameter of 1 mm at an extrusion rate of 1000 mm/min and an extrusion temperature of 170 °C. A water bath and a winder with 70 mm in diameter were placed at a distance of 520 mm and 810 mm from the spinneret exit, respectively. The extruded gel fibers were cooled in a temperature-conditioned atmosphere and then quenched into a water bath for about 1 min, where the temperatures of the air atmosphere and water bath were controlled at 5 °C. The quenched fibers were then extracted in a *n*-hexane bath for 5 min to remove the residual decalin solvent. The extracted fiber specimens were then dried in air for 30 min to remove the remaining *n*-hexane solvent before any drawing run. The Designations and compositions of UHMWPE, UHMWPE/BC and UHMWPE/MBC as-prepared fiber specimens prepared in this study are summarized in Table 1.

2.2. Morphological analyses

In order to understand the morphologies on the surfaces of the BC, oxidized BC and MBC nanofibers prepared in "Materials and Sample Preparation" section, the BC, oxidized BC and MBC nanofibers were dispersed in alcohol and then dried onto a carbon-coated copper grid under ambient conditions prior to morphological and elemental analyses. The cast BC, oxidized BC and MBC nanofiber specimens were then examined using a Philip transmission electron microscope (TEM) model Tecnai G20 operated at 200 kV.

2.3. Specific surface area analyses

A Laser Particle Size Analyzer model BT-9300H (Dandong Bettersize Instruments Corporation, Dandong, China) was used to study the specific surface areas of the BC and MBC nanofibers prepared in the "Materials and sample preparation" section. Before analyses, ten micrograms of BC and MBC nanofibers were added and ultrasonicated in 10 ml decalin at 25 for 5 min, respectively. The specific surface areas of BC and MBC nanofibers were then measured by placing the ultrasonicated solutions prepared above in the curette of the Laser Particle Size Analyzer at 25.

2.4. Fourier transform infra-red spectroscopy

Fourier transform infra-red (FT-IR) spectroscopic measurements of the BC and MBC specimens were recorded on a Nicolet Avatar 360 FT-IR spectrophotometer at 25 °C, wherein 32 scans with a spectral resolution 1 cm^{-1} were collected during each spectroscopic measurement. Infra-red spectra of the BC and MBC film specimens were determined using the conventional KBr disk method. The BC and MBC nanofibers were cast onto KBr disk and dried at 60 °C for 30 min. The cast films used in this study were prepared sufficiently thin enough to obey the Beer–Lambert law.

2.5. Thermal, lamellar thickness and orientation factor analyses

The thermal properties of all samples were performed on a Du Pont differential scanning calorimeter (DSC) model 2000. All scans were carried out at a heating rate of 20 °C/min under flowing nitrogen at a flow rate of 25 ml/min. Samples weighing 0.5 mg and 15 mg were placed in the standard aluminum sample pans for determination of their melting temperature (T_m) and percentage crystallinity (X_c) values, respectively. The percentage crystallinity values of the as-prepared specimens were estimated using baselines drawn from 40 to 200 °C and a perfect heat of fusion of polyethylene of 293 J/g (Hoffman & Miller, 1997).

In order to understand the ultradrawing properties of UHMWPE, UHMWPE/BC, and UHMWPE/MBC as-prepared fiber specimens, the lamellar thickness (l_c) values of the above as-prepared fibers were evaluated from their T_m values using Hoffman and Week's equation (Hoffman & Miller, 1997; Hoffman & Weeks, 1962) given as follows. In which, an equilibrium melting temperature (T_m^0) of 145.5 °C, a perfect heat of fusion (ΔH_f^0) of 293 J/g and a folded surface free energy (σ_e) of 9×10^{-6} J/cm^2 of polyethylene crystals (Hoffman & Miller, 1997) were used for evaluation of l_c values of UHMWPE, UHMWPE/BC, and UHMWPE/MBC as-prepared fiber specimens.

$$T_m = T_m^0 \left[1 - \frac{2\sigma_e}{l_c \Delta H_f^0} \right] \tag{1}$$

The orientation factor (f_o) values of UHMWPE, UHMWPE/BC, and UHMWPE/MBC as-prepared and drawn fiber specimens were measured using a sonic velocity orientation instrument model SCY-III, which was purchased from Donghuakaili Chemicals and Fiber Technology Corporation, Shanghai, China. Before testing, the fiber specimen with 60 cm in length was wound and clamped on a testing device with a span of 40 cm. The f_o values of the as-spun and drawn fiber specimens were then measured at 25 °C. A minimum of five samples of each specimen were tested and averaged during the orientation measurements. The f_o values were evaluated using Eq. (2) as suggested by Xiao, Zhang, An, and Jia (1997):

$$f_s = 1 - \left(\frac{C_u}{C} \right)^2 \tag{2}$$

where C is the sonic velocity of the as-prepared or drawn UHMWPE fiber specimen and C_u is the sonic velocity of the fully unoriented sample, taken as 1.65 km/s (Xiao et al., 1997).

2.6. Drawing and tensile properties of the fiber specimens

The UHMWPE, UHMWPE/BC, and UHMWPE/MBC fiber specimens used in the drawing experiments were cut from the dried as-prepared fibers and then stretched on a Gotech tension testing machine model GT-TFS-2000 equipped with a temperature-controlled oven. The fibers are 20 mm in length, which were wound and clamped in a stretching device and then stretched at a crosshead speed of 20 mm/min and a constant temperature of 95 °C. The draw ratio of each fiber specimen was determined as the ratio of the marked displacement after and before drawing. The marked displacement before drawing was 27 mm. The tensile properties of the as-prepared and drawn fibers were also determined using a Hung-Ta tension testing machine model HT-9112 at a crosshead speed of 20 mm/min. A minimum of five samples of each specimen were tested and averaged during the tensile experiments.

Table 1
Designations and compositions of UHMWPE, UHMWPE/BC, and UHMWPE/MBC as-prepared fiber specimens.

As-prepared fiber specimens	UHMWPE (g/phr)	BC (g/phr)	MBC (g/phr)	Volumes of decalin in gel solutions (ml)
F_{100}	2/100	0	0	100
$F_{100}BC_{0.0125}$	2/100	0.00025/0.0125	–	100
$F_{100}BC_{0.025}$	2/100	0.0005/0.025	–	100
$F_{100}BC_{0.0375}$	2/100	0.00075/0.0375	–	100
$F_{100}BC_{0.05}$	2/100	0.001/0.05	–	100
$F_{100}BC_{0.0625}$	2/100	0.00125/0.0625	–	100
$F_{100}BC_{0.075}$	2/100	0.0015/0.075	–	100
$F_{100}BC_{0.1}$	2/100	0.002/0.1	–	100
$F_{100}MBC_{1-0.0125}$	2/100	–	0.00025/0.0125	100
F_{100} $MBC_{1-0.025}$	2/100	–	0.0005/0.025	100
F_{100} $MBC_{1-0.0375}$	2/100	–	0.00075/0.0375	100
F_{100} $MBC_{1-0.05}$	2/100	–	0.001/0.05	100
F_{100} $MBC_{1-0.0625}$	2/100	–	0.00125/0.0625	100
F_{100} $MBC_{1-0.075}$	2/100	–	0.0015/0.075	100
F_{100} $MBC_{1-0.1}$	2/100	–	0.002/0.1	100
$F_{100}MBC_{2-0.0125}$	2/100	–	0.00025/0.0125	100
F_{100} $MBC_{2-0.025}$	2/100	–	0.0005/0.025	100
F_{100} $MBC_{2-0.0375}$	2/100	–	0.00075/0.0375	100
F_{100} $MBC_{2-0.05}$	2/100	–	0.001/0.05	100
F_{100} $MBC_{2-0.0625}$	2/100	–	0.00125/0.0625	100
F_{100} $MBC_{2-0.075}$	2/100	–	0.0015/0.075	100
F_{100} $MBC_{2-0.1}$	2/100	–	0.002/0.1	100
$F_{100}MBC_{3-0.0125}$	2/100	–	0.00025/0.0125	100
F_{100} $MBC_{3-0.025}$	2/100	–	0.0005/0.025	100
F_{100} $MBC_{3-0.0375}$	2/100	–	0.00075/0.0375	100
F_{100} $MBC_{3-0.05}$	2/100	–	0.001/0.05	100
F_{100} $MBC_{3-0.0625}$	2/100	–	0.00125/0.0625	100
F_{100} $MBC_{3-0.075}$	2/100	–	0.0015/0.075	100
F_{100} $MBC_{3-0.1}$	2/100	–	0.002/0.1	100
$F_{100}MBC_{4-0.0125}$	2/100	–	0.00025/0.0125	100
F_{100} $MBC_{4-0.025}$	2/100	–	0.0005/0.025	100
F_{100} $MBC_{4-0.0375}$	2/100	–	0.00075/0.0375	100
F_{100} $MBC_{4-0.05}$	2/100	–	0.001/0.05	100
F_{100} $MBC_{4-0.0625}$	2/100	–	0.00125/0.0625	100
F_{100} $MBC_{4-0.075}$	2/100	–	0.0015/0.075	100
F_{100} $MBC_{4-0.1}$	2/100	–	0.002/0.1	100

3. Results and discussion

3.1. Morphological analyses of the original, oxidized and modified BC nanofibers

Fig. 1 exhibits typical TEM micrographs of original, oxidized and modified BC nanofiber specimens. Typical reticulated rodlike feature with dimensions of 0.1–1 μm in length and 20–80 nm in diameter was observed for both original and oxidized BC nanofiber specimens (see Fig. 1a and b). After oxidation by $NaIO_4$ solutions, the translucent impurities original present in between BC nanofibers were removed and the oxidized BC nanofibers are significantly thinner than original BC nanofibers (see Fig. 1b). After being modified by $PE_{\text{-g-MAH}}$, some translucent resins were found attaching on the surface of the BC nanofibers, wherein the amounts of attached translucent resins increased gradually as the weight ratios of $PE_{\text{-g-MAH}}$ to BC nanofibers increase (see Fig. 1c–f). The attached translucent resins were most likely the grafted $PE_{\text{-g-MAH}}$ molecules, which were firmly bonded to BC nanofibers by the reaction of the maleic anhydride groups of $PE_{\text{-g-MAH}}$ with the hydroxyl groups of the BC nanofibers. In fact, the translucent resins were found fully surrounding and overwrapping on BC nanofibers, as the weight ratios of $PE_{\text{-g-MAH}}$ to BC nanofibers are equal to or more than 10.

3.2. Fourier transform infra-red spectroscopy

Fig. 2 illustrates typical Fourier transform infra-red (FT-IR) spectra of original bacterial cellulose (BC), modified bacterial cellulose (MBC), and maleic anhydride grafted polyethylene ($PE_{\text{-g-MAH}}$) specimens. As shown in Fig. 2a, six distinctive absorption bands centered at 1065, 1160, 1375, 1644, 2921 and 3380 cm^{-1} corresponding to the motions of C—O stretching (Smidt, Lechner, Schwanninger, Haberhauer, & Gerzabek, 2002), —OH wagging (Liang & Marchessault, 1959), C—H scissor (Belousova, Shablygin, Belousova, Golova, & Papkov, 1986), H—O—H stretching (Belousova et al., 1986), $—CH_2$ stretching (Qiuying, Xinyuan, & Xinkun, 2011) and —OH stretching vibrations (Embuscado et al., 1994), respectively, were found on the FT-IR spectrum of the BC specimen. The $PE_{\text{-g-MAH}}$ specimen exhibited two distinctive absorption bands centered at 1711 and 1791 cm^{-1}, which were generally attributed to the motion of O—C=O and C=O stretching vibrations of maleic anhydride (Sawatari et al., 1986) (see Fig. 2f).

After modification, the peak magnitudes corresponding to —OH stretching bands of MBC specimens reduce significantly as the weight ratios of $PE_{\text{-g-MAH}}$ to BC nanofibers increase (see Fig. 2b–e). In fact, as shown in Fig. 2e, the —OH stretching bands originally present in BC specimen disappear almost completely as the weight ratios of $PE_{\text{-g-MAH}}$ to BC nanofibers of MBC specimens are equal to 15. On the other hand, two newly absorption bands centered at 1068, 1164 and 1735 cm^{-1}, corresponding to the motion of ester C—O and C=O stretching vibration, respectively were found in the spectra of MBC_1, MBC_2, MBC_3 and MBC_4 specimens (see Fig. 2b–e). The newly developed ester C—O and C=O stretching bands and/or gradually disappeared —OH stretching bands of MBC specimens is attributed to the reaction of the hydroxyl groups of BC nanofibers with the maleic anhydride groups of $PE_{\text{-g-MAH}}$ molecules during their modification processes. In contrast, the absorption band centered at 1711 and 1791 cm^{-1} corresponding to the motions of

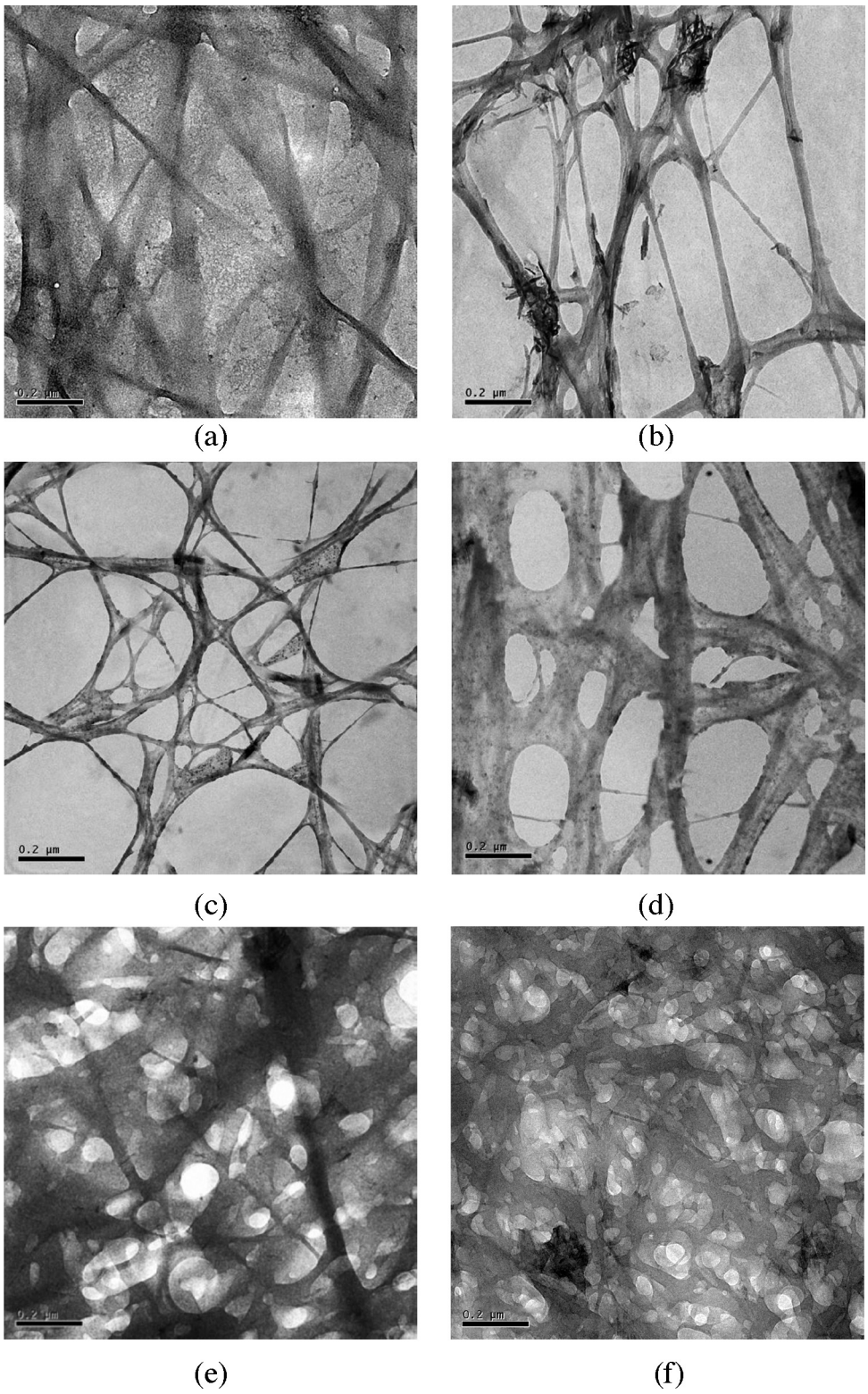

Fig. 1. TEM micrographs of (a) BC, (b) oxidized BC, (c) MBC_1, (d) MBC_2, (e) MBC_3 and (f) MBC_4 nanofiber specimens.

O—C=O and C=O stretching vibrations of maleic anhydride reappeared as the weight ratios of $PE_{-g\text{-}MAH}$ to BC nanofibers of MBC specimens are equal to 15. The reappearance of O—C=O and C=O stretching bands of maleic anhydride groups is most likely due to the over-dosage of $PE_{-g\text{-}MAH}$ during the preparation processes of MBC specimens.

3.3. Specific surface area analyses of BC and MBC nanofibers

The values of specific surface areas of BC and MBC nanofibers are summarized in Table 2. The specific surface area of the BC nanofiber specimen reaches an extraordinary high value at 393.7 m^2/g. After modification, the specific surface areas of MBC nanofiber specimens

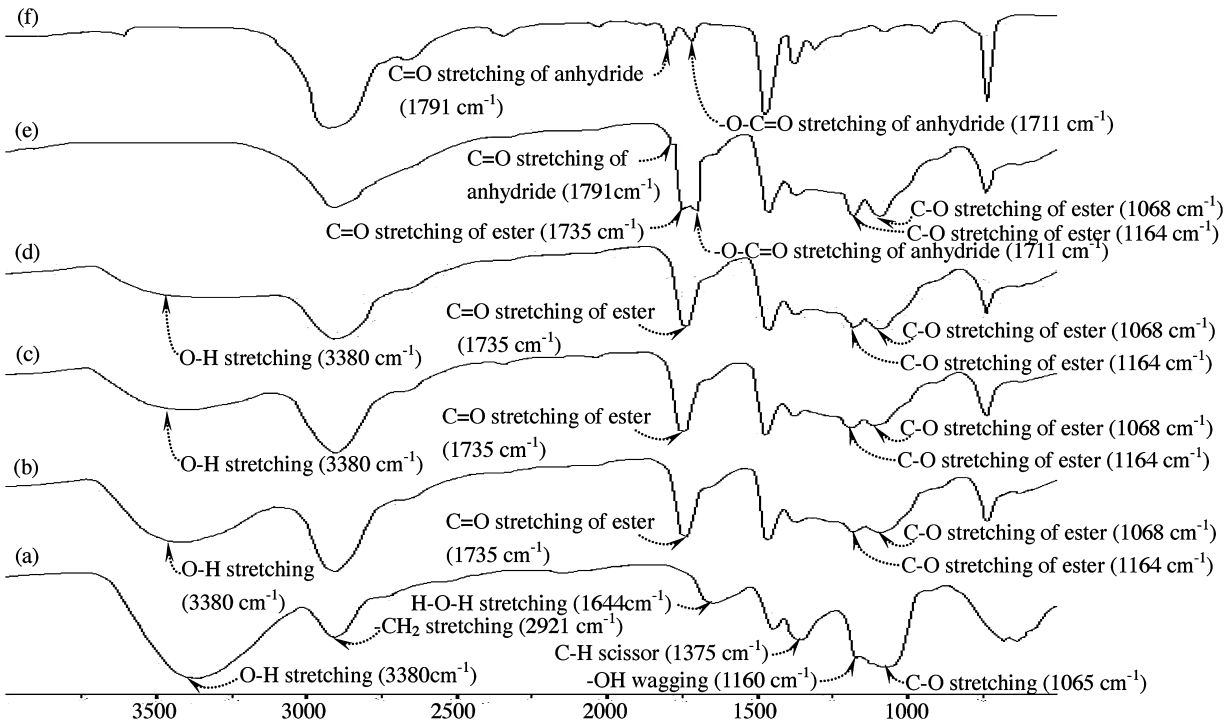

Fig. 2. FT-IR spectra of (a) bacterial cellulose, (b) MBC1, (c) MBC2, (d) MBC3, (e) MBC4 modified bacterial cellulose, and (f) maleic anhydride grafted Polyethylene specimens.

are significantly higher than that of the BC nanofiber specimen. In fact, the specific surface areas of MBC specimens increase significantly with the increase in PE_{-g-MAH} contents and reach a maximal value at 439.7 m^2/g as the weight ratios of PE_{-g-MAH} to BC approach an optimal value at 10. Conversely, the specific surface areas of the MBC nanofiber specimens reduce from 439.7 to 435.9 m^2/g, as their weight ratios of PE_{-g-MAH} to BC increase from 10 to 15.

Presumably, the beneficial effect of PE_{-g-MAH} contents on specific surface areas of MBC nanofiber specimens is attributed to the increase in grafted amounts and specific surface areas of PE_{-g-MAH} on BC nanofibers during their modification processes. However, PE_{-g-MAH} molecules may agglomerate, bundle, entangle together and overwrap the BC nanofibers, as PE_{-g-MAH} molecules are present in excess amounts that can no longer grafted onto the BC nanofibers. As evidenced by morphology analyses in the previous section, some translucent resins were found fully surrounding and overwrapping on BC nanofibers, as the weight ratios of PE_{-g-MAH} to BC nanofibers are more than 10. Based on this premise, it is reasonable to infer that the overwrapped BC nanofibers exhibit relatively lower specific surface areas than those MBC nanofibers grafted with proper amounts of PE_{-g-MAH} molecules.

3.4. Thermal properties of the as-prepared fibers

Typical DSC thermograms of UHMWPE (F_{100}), UHMWPE/BC ($F_{100}BC_y$) and UHMWPE/MBC ($F_{100}MBC_{x-y}$) as-prepared fiber series specimens are summarized in Fig. 3. The lamellar thickness (l_c) values of F_{100}, $F_{100}BC_y$ and $F_{100}MBC_{x-y}$ as-prepared fiber specimens evaluated from their melting temperature (T_m) values using Hoffman and Week's equation (Hoffman & Miller, 1997; Hoffman & Weeks, 1962) are also summarized in Fig. 3. A main melting endotherm with a peak melting temperature (T_m) and percentage crystallinity (X_c) at 139.6 °C and 65.8%, respectively, was found for the UHMWPE as-prepared fiber specimen (i.e. F_{100} specimen). After incorporation of BC nanofibers in UHMWPE, the T_m (or l_c) and X_c values of $F_{100}BC_y$ as-prepared fiber specimens remain nearly at the same value, respectively, as their BC contents increase (see Figs. 3a–d). In contrast, the T_m (or l_c) and X_c values of each $F_{100}MBC_{x-y}$ as-prepared fiber series specimens approach the minimal and maximal values, respectively, as their MBC contents reach an optimal value at 0.0625 phr. For instance, T_m(or evaluated l_c) and X_c values of $F_{100}MBC_{1-0.0625}$ as-prepared fiber specimen are 136.3 °C (or 10.1 nm) and 73.1%, which are about 0.5–1.3 °C (or 0.6–1.7 nm) lower and 0.3–3.8% higher than those of other corresponding $F_{100}MBC_{1-y}$ as-prepared fiber specimens prepared with MBC_1 contents other than the optimal value at 0.0625 phr. Moreover, it is worth noting that $F_{100}MBC_{3-0.0625}$ as-prepared fiber specimen exhibit the lowest T_m (or evaluated l_c) and the highest X_c values among the $F_{100}MBC_{x-0.0625}$ as-prepared fiber series specimens prepared with the same optimal MBC content but modified with weight ratios of PE_{-g-MAH} to BC other than 10 (see Fig. 3).

As evidenced by the specific surface area and TEM analyses, the BC and MBC nanofibers are with relatively large surface areas per volume, which make them in close proximity to a large fraction of the UHMWPE matrix. Apparently, even small contents of dispersed MBC nanofibers can serve as efficient nucleation sites for UHMWPE molecules during their gel-spinning processes. These efficient nucleation sites of MBC nanofibers then facilitate the crystallization of UHMWPE molecules into crystals with thinner lamellar thickness and/or lower T_m values during their gel-spinning processes. However, the highly polar and reticulated BC nanofiers appeared to agglomerate and bundle together in UHMWPE matrix, and did not serve as an effective nucleating agent during the gel-spinning

Table 2
Designations and specific surface areas of BC and MBC specimens prepared in this study.

Bacterial cellulose and modified bacterial cellulose specimens	Mass ratios of PE_{g-MAH} to BC	Specific surface area (m^2/g)
BC	0	393.7
MBC_1	2	425.3
MBC_2	5	435.6
MBC_3	10	439.7
MBC_4	15	435.9

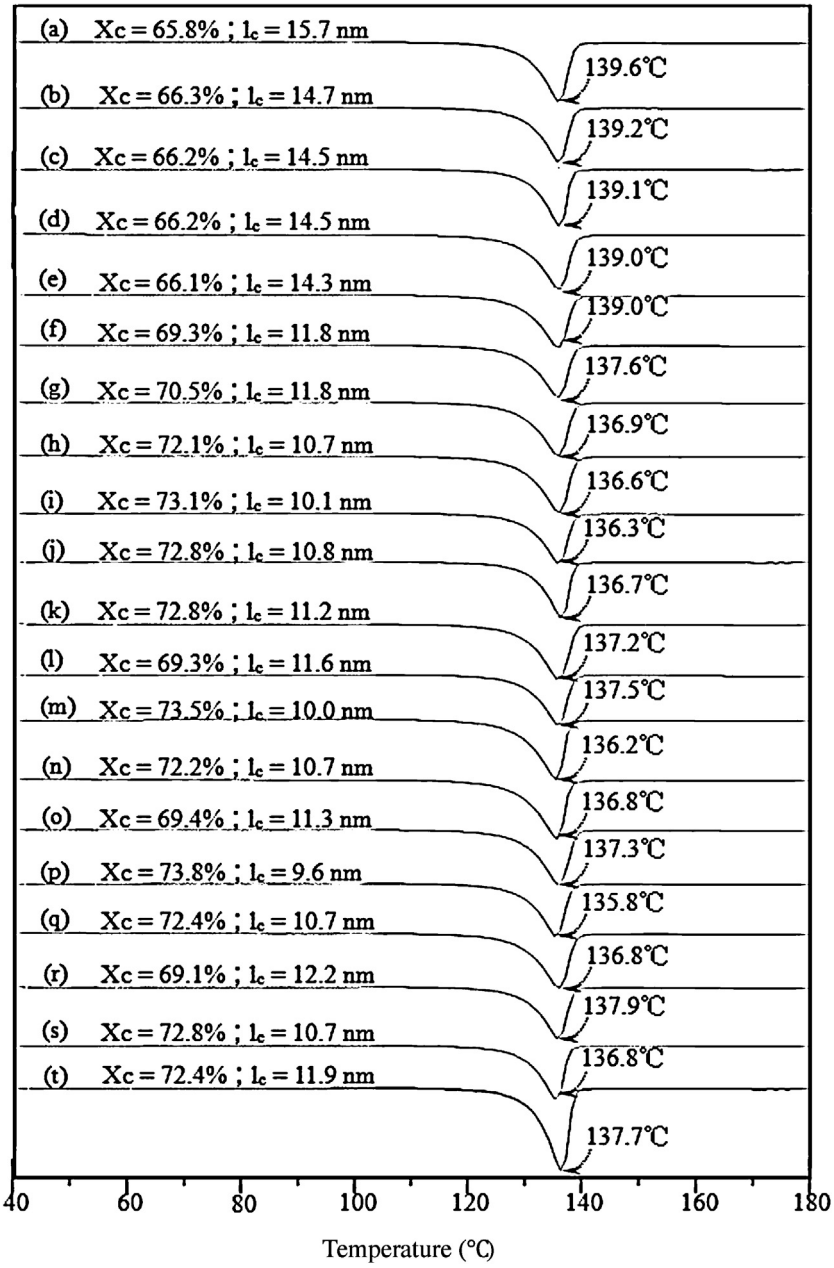

Fig. 3. DSC thermograms of (a) F100, (b) F100BC0.0125, (c) F100BC0.025, (d), F100BC0.0625, (e) F100BC0.1, (f) F100MBC1–0.0125, (g) F100MBC1–0.025, (h), F100MBC1–0.05, (i) F100MBC1–0.0625, (j) F100MBC1–0.075, (k) F100MBC1–0.1, (l), F100MBC2–0.0125, (m) F2MBC2–0.0625, (n) F100MBC2–0.1, (o) F100MBC3–0.0125, (p) F100MBC3–0.0625, (q) F100MBC3–0.1, (r) F100MBC4–0.0125, (s) F100MBC4–0.0625 and (t) F100MBC4–0.1.

processes of UHMWPE/BC fibers. As a consequence, $F_{100}MBC_{x-y}$ as-prepared fiber specimens exhibit significantly higher X_c but lower T_m (or evaluated l_c) values than the corresponding $F_{100}BC_y$ as-prepared fiber specimens prepared with the same BC contents but without modification.

3.5. Orientation factor analyses of the as-prepared and drawn fiber specimens

Typical orientation factor (f_o) values of F_{100}, $F_{100}BC_y$ and $F_{100}MBC_{x-y}$ as-prepared and drawn fiber specimens are summarized in Fig. 4. As shown in Fig. 4, no significant difference in f_o values was found for F_{100}, $F_{100}BC_y$ and $F_{100}MBC_{x-y}$ as-prepared fiber specimens. As expected, f_o values of F_{100}, $F_{100}BC_y$ and $F_{100}MBC_{x-y}$ fiber series specimens increase consistently as their draw ratios increase. After addition of MBC nanofibers, the f_o values of drawn $F_{100}MBC_{-y}$ fiber specimens are significantly higher than those of F_{100} and $F_{100}BC_y$ fiber specimens with the same draw ratios. The f_o values of each drawn $F_{100}MBC_{x-y}$ fiber series specimens reach a maximal value as their MBC contents approach an optimal value at 0.0625 phr. In which, the maximum f_o values obtained for drawn $F_{100}MBC_{x-0.0625}$ fiber specimens prepared at the optimal MBC content reach another maximum value as the weight ratios of $PE_{-g\text{-}MAH}$ to BC approach an optimal value at 10 (see Fig. 4).

3.6. Achievable draw ratios of the as-prepared fiber specimens

Fig. 5 summarized the achievable draw ratio (D_{ra}) values of F_{100}, $F_{100}BC_y$ and $F_{100}MBC_{x-y}$ as-prepared fiber specimens prepared at varying BC and/or MBC contents. Regardless of the BC contents,

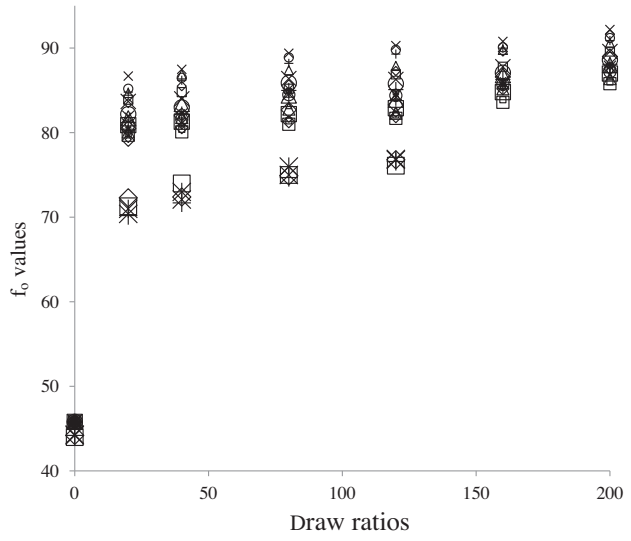

Fig. 4. The orientation factor (f_o) values of F100 (*), F100BC0.0125 (□), F100BC0.025, (◊), F100BC0.0625 (×), F100BC0.1 (+), F100MBC1−0.0125 (□), F100MBC1−0.025 (◊), F100MBC1−0.05 (Δ), F100MBC1−0.0625 (×), F100MBC1−0.075 (○), F100MBC1−0.1 (+), F100MBC2−0.0125 (□), F100MBC2−0.025 (◊), F100MBC2−0.05 (Δ), F100MBC2−0.0625 (×), F100MBC2−0.075 (○), F100MBC2−0.1 (+), F100MBC3−0.0125 (□), F100MBC3−0.025 (◊), F100MBC3−0.05 (Δ), F100MBC3−0.0625 (×), F100MBC3−0.075 (○), F100MBC3−0.1 (+), F100MBC4−0.0125 (□), F100MBC4−0.025 (◊), F100MBC4−0.05 (Δ), F100MBC4−0.0625 (×), F100MBC4−0.075 (○) and F100MBC4−0.1 (+) as-prepared and drawn fiber specimens with varying draw ratios.

the D_{ra} values of $F_{100}BC_y$ as-prepared fiber specimens remain relatively unchanged at about 130, which are about the same value as that of the F_{100} as-prepared fiber specimen without addition of BC nanofibers. After incorporation of MBC nanofibers in UHMWPE, the D_{ra} values of each F_2MBC_{x-y} fiber series specimens improve significantly with the initial increase in MBC contents, and then reach a maximal value as their MBC contents approach an optimal value at 0.0625 phr. In which, the maximum D_{ra} value obtained for $F_{100}MBC_{3-0.0625}$ as-prepared fiber specimen prepared at the optimal MBC content are significantly higher than those of the corresponding $F_{100}MBC_{x-0.0625}$ as-prepared fiber specimens with MBC modified with weight ratios of PE_{-g-MAH} to BC other than 10. In fact, as shown in Fig. 5, the maximal D_{ra} value obtained for $F_{100}MBC_{3-0.0625}$ as-prepared fiber specimen is about 2.6 times

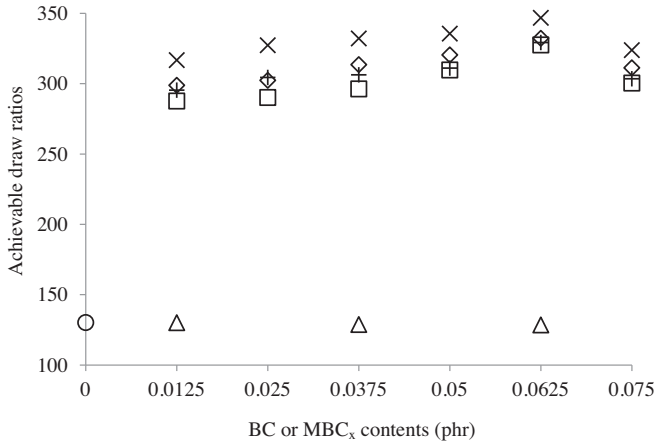

Fig. 5. Achievable draw ratios of F100 (○), F100BCx (Δ), F100MBC1−y (□), F100MBC2−y (◊), F100MBC3−y (×) and F100MBC4−y (†) as-prepared fiber specimens.

of the D_{ra} values of F_{100} and $F_{100}BC_y$ as-prepared fiber specimens (348.2 vs. 130).

As evidenced by thermal and lamellar thickness analyses, the T_m and/or evaluated l_c values of $F_{100}MBC_{x-y}$ as-prepared fiber specimens reduce significantly with the increase in MBC contents, although the amounts of crystals with lower T_m and/or evaluated l_c values increase significantly as their MBC contents increase to the optimal value. Presumably, these crystals with lower T_m and/or evaluated l_c values can be melted and pulled out of folded lamellar crystals relatively easily during the ultradrawing processes, and hence, results in higher drawability and orientation of the $F_{100}MBC_{x-y}$ fibers. However, the amounts of coagulated MBC nanofibers are likely to increase when their MBC contents are higher than certain values. These coagulated MBC nanofibers can slide against each other and serve as the defects for stress concentration during the drawing processes of $F_{100}MBC_{x-y}$ as-prepared fiber specimens, and hence lead to an early breakage and/or significant reduction in the D_{ra} and f_o values of the resulted drawn fibers. Based on these premises, it is reasonable to understand that the D_{ra} values of $F_{100}MBC_{x-y}$ as-prepared fiber specimens and f_o values of the drawn $F_{100}MBC_{x-y}$ fiber specimens with a fixed draw ratio reduce significantly when their MBC contents are higher than the specific optimal value.

3.7. Tensile properties

The tensile properties of F_{100}, $F_{100}BC_y$ and $F_{100}MBC_{x-y}$ as-preparedfiber series specimens prepared at varying draw ratios are illustrated in Fig. 6. As expected, the tensile strength (σ_f) and modulus (E) values of the drawn F_{100}, $F_{100}BC_y$ and $F_{100}MBC_{x-y}$ fiber series specimens improve consistently as their draw ratios increase. It is worth noting that σ_f and E values of the drawn $F_{100}MBC_{x-y}$ fiber series specimens are significantly higher than those of the corresponding drawn F_{100} and/or $F_{100}BC_y$ fiber specimens with the same draw ratio but without addition of modified BC nanofibers. In which, the σ_f and E values of the drawn $F_{100}BC_y$ fiber specimens are only slightly higher than those of the corresponding F_{100} fiber specimens prepared at the same draw ratios but without addition of BC nanofibers. Similar to those found for their f_o, σ_f and E values of each drawn $F_{100}MBC_{x-y}$ fiber series specimens with a fixed draw ratio approach a maximum value as their MBC contents near the optimal value at 0.0625 phr. In which, the σ_f and E values of the drawn $F_{100}MBC_{3-y}$ fiber specimens are significantly higher than those of the corresponding $F_{100}MBC_{x-y}$ fiber specimens prepared at the same draw ratios and MBC contents but with MBC modified with weight ratios of PE_{-g-MAH} to BC other than 10.

The mechanical properties of the drawn specimens are generally believed to depend mainly on the degree of orientation of the drawn specimens, as their molecular weights are constant (Hoogsteen, ten Brinke, & Pennings, 1988; Ohta, 1983). As evidenced by orientation analyses in the previous section, the f_o values of the $F_{100}MBC_{x-y}$ fiber specimens are always higher than those of the F_{100} fiber specimens with the same draw ratios, and/or corresponding $F_{100}BC_y$ fiber specimens with the same draw ratios and BC contents. Moreover, at a fixed draw ratio, the f_o values of drawn $F_{100}MBC_{x-0.0625}$ fiber specimens prepared at the optimal MBC contents are always higher than those of other corresponding $F_{100}MBC_{x-y}$ fiber specimens prepared with the same type of MBC but with contents other than the optimal content at 0.0625 phr, respectively. These results clearly suggest that a good orientation of UHMWPE molecules along the drawing direction positively affects the tensile properties of the $F_{100}BC_y$ and $F_{100}MBC_{x-y}$ fiber specimens. Excellent orientation and tensile properties of the UHMWPE fibers can be prepared by ultradrawing the $F_{100}MBC_{x-y}$ as-prepared fibers with the optimal MBC contents well dispersing in $F_{100}MBC_{x-y}$ as-prepared fibers.

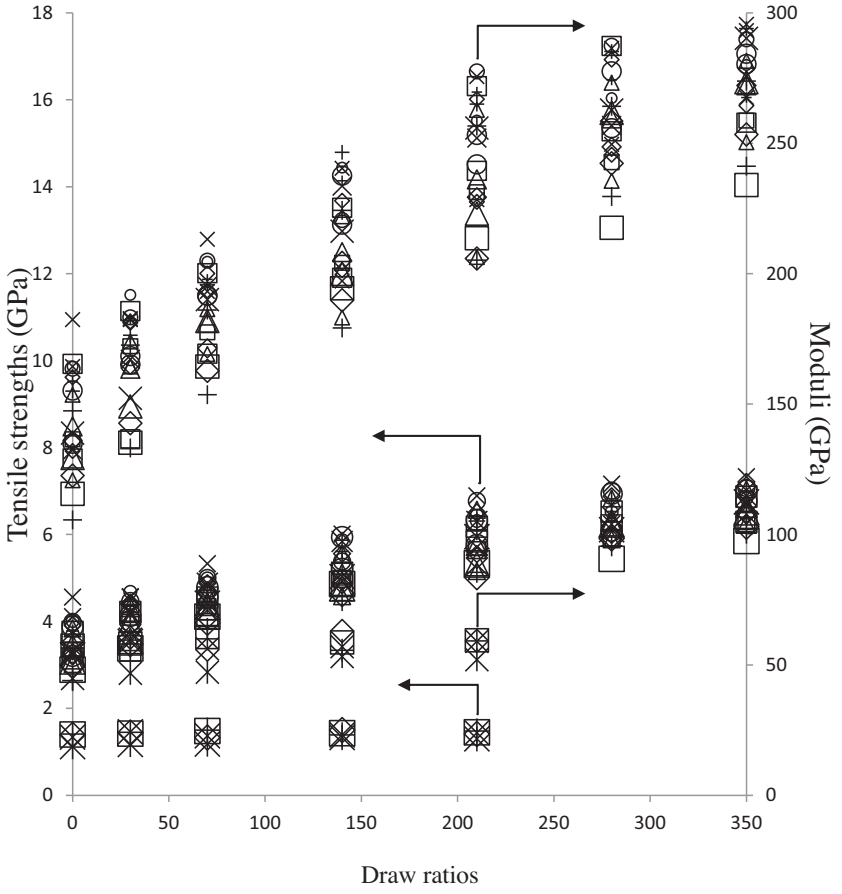

Fig. 6. The tensile strength values and modulus values of F100 (*, *), F100BC0.0125, (□,□), F100BC0.025 (◊,◊), F100BC0.0625 (×, ×), F100BC0.1 (+, +), F100MBC1−0.0125, (□,□), F100MBC1−0.025 (◊,◊), F100MBC1−0.05 (Δ, Δ), F100MBC1−0.0625 (×, ×), F100MBC1−0.075 (○, ○), F100MBC1−0.1 (++), F100MBC2−0.0125 (□,□), F100MBC2−0.025, (◊,◊), F100MBC2−0.05 (Δ, Δ), F100MBC2−0.0625 (×, ×), F100MBC2−0.075 (○, ○), F100MBC2−0.1 (+, +), F100MBC3−0.0125 (□,□), F100MBC3−0.025 (◊,◊), F100MBC3−0.05 (Δ, Δ), F100MBC3−0.0625 (×, ×), F100MBC3−0.075 (○, ○), F100MBC3−0.1 (+,+), F100MBC4−0.0125 (□,□), F100MBC4−0.025 (◊,◊), F100MBC4−0.05 (Δ, Δ), F100MBC4−0.0625 (×, ×), F100MBC4−0.075 (○, ○) and F100MBC4−0.1 (+,+) fiber specimens with varying draw ratios.

4. Conclusions

As evidenced by FTIR and TEM analysis, $PE_{\text{-g-MAH}}$ molecules were successfully grafted onto modified BC nanofibers through the reaction of the hydroxyl groups of BC nanofibers with the maleic anhydride groups of $PE_{\text{-g-MAH}}$ molecules during their modification processes. The specific surface areas of the MBC nanofibers reached a maximum value at 439.7 m^2/g as the weight ratios of $PE_{\text{-g-MAH}}$ to BC nanofibers approached the optimal value at 10. After incorporation of MBC nanofibers in UHMWPE, T_m and evaluated l_c values of $F_{100}MBC_{x-y}$ as-prepared fiber series specimens reduce, but X_c values increase significantly, as their MBC contents increase to the optimal value at 0.0625 phr. In which, T_m, l_c and X_c values of the $F_{100}BC_y$ as-prepared fiber specimens with varying BC contents are nearly the same as those of the F_{100} as-prepared fiber specimen. Apparently, the small contents of MBC nanofibers serve as efficient nucleation sites and facilitate the crystallization of UHMWPE molecules into crystals with lower T_m and l_c values during their gel-spinning processes. The well dispersed MBC nanofibers with even higher specific surface areas are likely to serve as more effective sites for nucleation of UHMWPE molecules during their gel-spinning processes than the BC nanofibers. The D_{ra} values of each $F_{100}MBC_{x-y}$ as-prepared fiber series specimens approached a maximum value as the MBC contents reached the optimal value at 0.0625 phr. In which, the maximum D_{ra} value obtained for $F_{100}MBC_{x-0.0625}$ as-prepared fiber specimen prepared at the optimal MBC content reached another maximum value as the weight ratio of $PE_{\text{-g-MAH}}$ to BC approach an optimal value at 10. Similar to those found for the achievable drawing properties of the $F_{100}MBC_{x-y}$ as-prepared fibers, the f_o, σ_f and E values of drawn $F_{100}MBC_{x-y}$ fiber series specimens with a fixed draw ratio reach a maximum value as their MBC contents approach the optimal value, wherein the σ_f and E values of the drawn $F_{100}MBC_{x-y}$ fiber specimens are always significantly higher than those of the drawn F_{100} fiber specimens and corresponding drawn $F_{100}BC_y$ fiber specimens prepared at the same draw ratios and BC contents but without being modified. Similarly, the f_o, σ_f and E values of the drawn $F_{100}MBC_{x-0.0625}$ fiber specimen with a fixed draw ratio reached another maximum value as the weight ratio of $PE_{\text{-g-MAH}}$ to BC nanofibers approach the optimal value at 10. The above results suggest that excellent orientation and tensile properties of the UHMWPE nanocomposite fibers can be obtained by ultradrawing the $F_{100}MBC_{x-y}$ as-prepared fibers with the optimal contents and well dispersed modified BC nanofibers.

Acknowledgements

The authors would like to express their appreciation to the Department of Industrial Technology, Ministry of Economic Affairs (95-EC-17-A-11-S1-057, 96-EC-17-A-11-S1-057, 97-EC-17-A-11-S1-057, 99-EC-17-A-11-S1-155 and 100-EC-17-A-11-S1-155), Taiwan Textile Research Institute and National Science Council (NSC 95-2221-E-253-008-MY3 and NSC 99-2221-E-011-010-MY3) for support of this work.

References

Abo, M. I., Maaty, E. I., Olley, R. H., & Bassett, D. C. (1999). *Journal of Materials Sciences*, *34*, 1975.
Belousova, T. A., Shablygin, M. V., Belousova, Y. Y., Golova, L. K., & Papkov, S. P. (1986). *Polymer Science*, *28*, 1115.
Cha, W. I., Hyon, S. H., & Ikada, Y. (1994). *The Journal of Polymer Science Part B: Polymer Physics*, *32*, 297.
Choi, N. W., Mori, I., & Ohama, Y. (2006). *Waste Management*, *26*, 189.
Cristian, J. G., Fernando, G. T., Clara, M. G., Omar, P. T., Josep, C. F., Cristian, J. G., et al. (2009). *Materials Science and Engineering*, *29*, 1098.
Cyras, V. P., Lannace, S., Kenny, J. M., & Vazquez, A. (2001). *Polymer Composites*, *22*, 104.
Darras, D., Sequela, R., & Rietsch, F. (1992). *Journal of Polymer Science: Polymer Physics Edition*, *30*, 349.
Embuscado, M. E., Marks, J. S., & BeMiller, J. N. (1994). *Food Hydrocolloids*, *8*, 407.
Gilkes, N. R., Kilburn, D. G., Miller, R. C., Jr., & Warren, R. A. J. (1991). *Bioresource Technology*, *36*, 21.
Hoffman, J. D., & Miller, R. L. (1997). *Polymer*, *38*, 3151.
Hoffman, J. D., & Weeks, J. J. (1962). *Journal of Research of the National Bureau of Standards*, *66*, 13.
Hoogsteen, W., ten Brinke, G., & Pennings, A. J. (1988). *Colloid and Polymer Science*, *266*, 1003.
Hwang, J. W., Yang, Y. K., Hwang, J. K., Pyun, Y. R., & Kim, Y. S. (1999). *Journal of Bioscience and Bioengineering*, *88*, 183.
Jiang, T., Lin, Y. T., Chen, K. N., & Yeh, J. T. (2003). *Polymer Engineering and Science*, *43*, 1765.
Joseph, K., Thomas, S., & Pavithran, C. (1996). *Polymer*, *37*, 5139.
Kajiwara, K., & Mcintyre, J. E. (1994). *Advanced fiber spinning technology*. Cambridge: Woodhead Publishing Ltd. Chapter 8.
Kalb, B., & Pennings, A. J. (1980a). *Journal of Materials Science*, *15*, 2548.
Kalb, B., & Pennings, A. J. (1980b). *Polymer*, *21*, 3.
Kanamoto, T., Tsurta, A., Tanana, K., Takeda, M., & Porter, R. S. (1988). *Macromolecules*, *21*, 470.
Kavesh, S., & Prevorsek, D. C. (1983) U.S. Patent 4413110.
Kavesh, S., & Prevorsek, D. C. (1985a) U.S. Patent 4536536.
Kavesh, S., & Prevorsek, D. C. (1985b) U.S. Patent 4551296.
Kurosumi, A., Sasaki, C., Yamashita, Y., & Nakamura, Y. (2002). *Carbohydrate Polymers*, *76*, 333.
Liang, C. Y., & Marchessault, R. H. (1959). *Polymer Science*, *37*, 385.
Matsuo, M., Sawatari, C., Iida, M., & Yoneda, M. (1985). *Polymer Journal*, *17*, 1197.
Mastuo, M., Sawatari, C., & Nakano, T. (1986). *Polymer Journal*, *18*, 759.
Ohta, T. (1983). *Polymer Engineering and Science*, *23*, 697.
Okiyama, A., Motoki, M., & Yamanaka, S. (1993). *Food Hydrocolloids*, *6*, 503.
Prevorsek, D. C. (1982). *Polymer liquid crystals*. Academic Press.
Qiuying, G., Xinyuan, S., & Xinkun, L. (2011). *Carbohydrate Polymers*, *83*, 1253.
Sawatari, C., Okumura, T., & Matsuo, M. (1986). *Polymer Journal*, *18*, 741.
Smidt, E., Lechner, P., Schwanninger, M., Haberhauer, G., & Gerzabek, M. H. (2002). *Applied Spectroscopy*, *56*, 1170.
Smith, P., & Lemstra, P. J. (1979). *Macromolecular Chemistry*, *180*, 2983.
Smith, P., & Lemstra, P. J. (1980a). *Journal of Materials Science*, *15*, 505.
Smith, P., & Lemstra, P. J. (1980b). *Polymer*, *21*, 1341.
Smith, P., Chanzy, H. D., & Rotzinger, B. P. (1985). *Polymer Communications*, *26*, 258.
Smith, P., Chanzy, H. D., & Rotzinger, B. P. (1987). *Journal of Materials Science*, *22*, 523.
Smook, J., & Pennings, A. J. (1982). *Journal of Applied Polymer Science*, *27*, 2209.
Suryanegara, L., Nakagaito, A. N., & Yano, H. (2009). *Composites Science and Technology*, *69*, 1187.
(1996). *Technical Textiles International*, *4*, 3.
Thwe, M. M., & Liao, K. (2002). *Composites Part A: Applied Science and Manufacturing*, *33*, 43.
Wan, Y. Z., Luo, H. L., He, F., Liang, H., Huang, Y., Wan, Y. Z., et al. (2009). *Composites Science and Technology*, *69*, 1212.
Wilding, M. A., & Word, I. M. (1978). *Polymer*, *19*, 969.
Xiao, H., Zhang, Y., An, S., & Jia, G. (1997). *Journal of Applied Polymer Science*, *59*, 931.
Yamanaka, S., Watanabe, K., Kitamura, N., Iguchi, M., Mitsuhashi, S., Yamanaka, S., et al. (1989). *Journal of Materials Science*, *24*, 3141.
Yamaura, K., Suzuki, M., Yamamoto, M., Shimada, R., & Tanigami, T. (1995). *Journal of Applied Polymer Science*, *58*, 1787.
Yamaura, K., Tanigami, T., Hayashi, N., Kosuda, K. I., Okuda, S., Yeh, J. T., et al. (1990). *Journal of Applied Polymer Science*, *40*, 905.
Yeh, J. T., & Chang, S. S. (2000). *Journal of Materials Science*, *35*, 3227.
Yeh, J. T., & Chang, S. S. (2001). *Journal of Applied Polymer Science*, *79*, 1890.
Yeh, J. T., & Chang, S. S. (2002). *Polymer Engineering and Science*, *42*, 1558.
Yeh, J. T., Chang, S. S., & Yen, M. S. (1998). *Journal of Applied Polymer Science*, *70*, 149.
Yeh, J. T., Du, C. W., Lin, S. C., Hsie, K. H., & Chang, F. C. (2008). *Journal of Materials Science*, *43*, 4892.
Yeh, J. T., Lai, Y. C., Liu, H., Shu, Y. C., Huang, C. Y., Yeh, J. T., et al. (2011). *Polymer International*, *60*, 59.
Yeh, J. T., Lin, Y. L., & Fan-Chiang, C. C. (1996). *Macromolecular Chemistry and Physics*, *197*, 3531.
Yeh, J. T., Lin, Y. T., & Chen, K. N. (2003a). *Journal of Applied Polymer Science*, *91*, 1559.
Yeh, J. T., Lin, Y. T., & Chen, K. N. (2003b). *Journal of Polymer Research*, *10*, 55.
Yeh, J. T., Lin, Y. T., & Chen, K. N. (2003c). *Journal of Applied Polymer Science*, *89*, 3728.
Yeh, J. T., Lin, S. C., Chen, K. N., & Huang, K. S. (2008). *Journal of Applied Polymer Science*, *110*, 2538.
Yeh, J. T., Wang, C. K., Hu, P., Lai, Y. C., & Tsai, F. C. (2012). *Polymer International*, *61*, 982.
Yeh, J. T., Wang, C. K., Yeh, A., Huang, L. K., Wang, W. H., Yeh, J. T., et al. (2013). *Polymer International*, *62*, 591.
Yeh, J. T., & Wu, H. C. (1998). *Polymer Journal*, *30*, 1.
Yeh, J. T., Wu, Z. W., Lai, Y. C., Li, Q. C., Hu, P., Yeh, J. T., et al. (2011). Polymer Engineering and Science. *51*, 2552.
Yeh, J. T., Wu, Z. W., Lai, Y. C., Zhou, H. P., Zhou, Q., Yeh, J. T., et al. (2011). *Polymer Engineering and Science*, *51*, 687.